

# Preliminary Results from an Interferometric Post-Coronagraph Wave Front Sensor<sup>12</sup>

J. Kent Wallace, Randall Bartos<sup>a</sup>, Paul Best<sup>a</sup>, B. Martin Levine<sup>a</sup>, Bijan Nemati<sup>a</sup>, Mike Shao<sup>a</sup>, Chris Shelton<sup>a</sup>

<sup>a</sup>Jet Propulsion Laboratory/California Institute of Technology

4800 Oak Grove Dr., Pasadena, CA 91109

818-393-7066

James.K.Wallace@jpl.nasa.gov

**Abstract**—In high contrast imaging system, semi-static, non-common path wave front errors not sensed by the active wave front sensor in an adaptive optics system will ‘leak’ around the coronagraph and lead to focal plane speckles that will mask exo-planets. Sensing and controlling these speckles is an absolute necessity for direct detection of planets from the ground. The next generation of AO systems that will enable direct detection of planets from the ground will become operational in the next couple of years. One of them, the Gemini Planet Imager, or GPI, will incorporate an interferometric wave front sensor, designed and developed at JPL, which will measure these errors. This talk will emphasize this novel sensor and describes how it is used to measure the non-common path amplitude and phase errors in the system that would otherwise limit the achievable contrast. We will describe the system error budget as well as simulations that model the system performance. The current status of the GPI Calibration System will be detailed, along with initial wavefront measurement results. This system promises a rich combination of interferometry and large optical systems in support of cutting edge science research.

implication for the abundance of planets in the universe is thrilling. However, direct detection of these planets remains a significant technical challenge due to the small angular separation and large difference in radiance. To date, the vast majority of detections have been made with indirect methods: the planet is inferred from the mutual effect of the planet/sun system upon each other. Direct detection would enable a more rapid determination of planetary companions and, with high-resolution astrometry, a more complete characterization of orbital parameters. Likewise, a detailed investigation of the spectral content of a planet’s light would lead to a greater understanding of its atmosphere including composition, temperature and gravity. There is much to be gained scientifically by detailed direct observations.

As mentioned previously, such observations are beset by several challenges: 1) the very small angular separation of the planet/star and 2) their significant contrast ratio. Challenging as these may be, new classes of coronagraphs and nulling interferometers have been proposed and developed over the last few years to address these concerns. The performance of these high-contrast instruments is now limited by residual systematic error sources. Image plane speckles (due to residual amplitude and phase errors that leak through the coronagraph or nullder) place severe constraints on what would otherwise be detectable.

The small phase and amplitude errors that produce these image plane speckles are neither perfectly static nor perfectly dynamic. If they were entirely static, they could be quantified by observing a calibrator star and simply subtracted from the final image. If they were perfectly dynamic, they would average to a halo that would become more uniform over time. Eventually, the faint planet would imprint itself upon the ever-smoother background. Instead, these image plane speckles tend to change over time scales of typical astronomical observations and so therefore don’t lend themselves to either classic calibration or averaging techniques. What has been heretofore lacking is a means of sensing and controlling (removing) these speckles during an observation.

## TABLE OF CONTENTS

1. INTRODUCTION.....	1
2. CALIBRATION WAVE FRONT SENSING IN	
CORONAGRAPHY .....	2
3. APPLICATION TO NULLING INTERFEROMETRY .....	3
4. CALIBRATION WAVE FRONT SENSOR TESTBED ..	3
5. PRELIMINARY RESULTS .....	4
6. FUTURE WORK.....	6
7. CONCLUSION .....	6
8. ACKNOWLEDGEMENTS .....	6
REFERENCES .....	6
BIOGRAPHY .....	6

## 1. INTRODUCTION

The shear number of known extra-solar planets detected is impressive ( $> 150$ ), and it continues to grow [2]. The

<sup>1</sup> U.S. Government work not protected by U.S. copyright

<sup>2</sup> IEEEAC paper #1378, Version 3, Updated December 18, 2007

The main goal of the calibration system for GPI is to sense these wave front errors and provide a measurement to the AO system so that they may be corrected. The calibration subsystem that will measure the mid-spatial frequency errors is called the high-order wave front sensor, HOWFS. Requisite contrasts for exo-planet detection are difficult, and GPI will have a suite of tools to bring to bear against the technical challenges. Centering of the star on the focal plane mask is one of these challenges, so as a separate task the calibration system will employ a low-order wave front sensor to establish the boresite of the instrument and ensure the centering is sufficient for achieving and maintaining high-contrast. This boresite will also be sufficiently accurate and stable for precision astrometry. This calibration subsystem is known as the low-order wave front sensor, or LOWFS.

## 2. CALIBRATION WAVE FRONT SENSING IN CORONAGRAPHY

The complex wave front that we expect from a high-contrast adaptive optics system (one with a large number of phase correcting elements and working at very fast sampling and update rates) has only small amplitude and phase errors and can therefore be expanded as follows:

$$E = Ae^{i\phi} \approx A(1 + \epsilon)(1 + i\varphi) \approx A + A(\epsilon + i\varphi) \quad (1)$$

Where  $A$  is the nominal magnitude of the electric field,  $\epsilon$  is a small fractional deviation from the nominal amplitude, and  $\varphi$  is the phase of the wavefront (here  $\varphi$  is a small fraction of a radian). Terms higher than second order in both the expansion and resulting simplification have been dropped. Transforming this slightly aberrant wave front to a

focal plane yields:

$$\Im[E] = \Im[A] + \Im[A(\epsilon + i\varphi)] = \text{Airy} + \Im[A(\epsilon + i\varphi)] \quad (2)$$

where  $\Im[\cdot]$  is the Fourier Transform operator. The effect of a classic coronagraph is to remove the Airy component of the above expression [3]. Re-imaging this coronagraph-filtered pupil results in an intensity distribution given by the following:

$$I_{\text{pupil}} \propto |A(\epsilon + i\varphi)|^2 = A^2(\epsilon^2 + \varphi^2) \quad (3)$$

Bright spots in this re-imaged pupil plane correspond to either residual phase or amplitude effects or a combination of both. With only a single image of the post-coronagraph pupil, it is impossible to definitively know if the pupil speckle is due to an amplitude or phase error. Introducing some phase diversity with a deformable mirror element that is conjugate to a bright spot would allow one to solve for the phase and amplitude contribution[4] (and minimize the phase contribution). However, doing so would reduce the observing efficiency of a high-contrast system, as this dithering would reduce the contrast in the final focal plane.

The confusion regarding the type of errors (phase or amplitude) in the above measurement and the magnitude of their contributions can be completely resolved in a much less disruptive way. Extracting a fraction of the light that would otherwise go to the science camera and interfering it with a reference wave front that is coherent with it [5,6,7]. This reference is conveniently available from the central core of the starlight that would otherwise be rejected by the coronagraph. An illustration of such an optical system is given above in Fig. 1.

After passing through the APLC, the electric field picks up

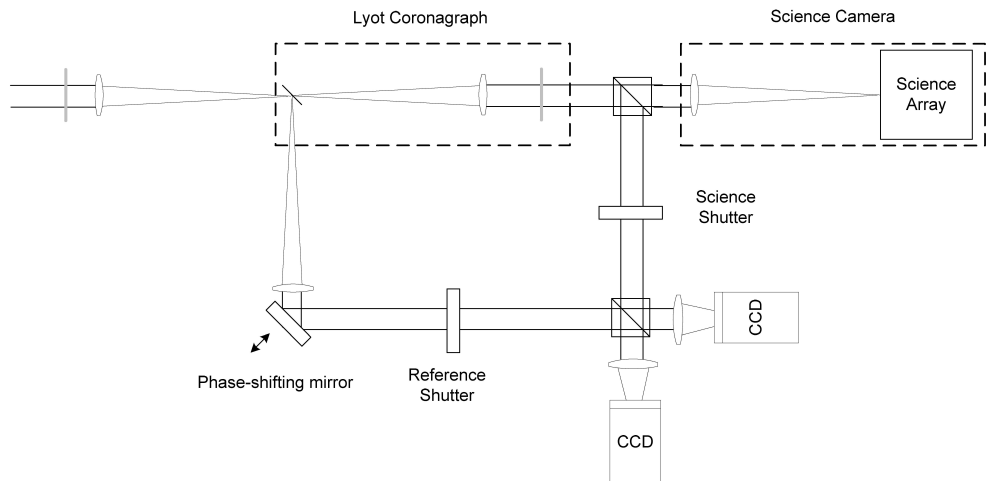


**Figure 1** – Simple cartoon illustrating the concept of interferometric wave front sensing in a coronagraph.

a pupil-dependent transmission:

$$(A + A(\varepsilon + i\varphi)) t_{APLC}(x, y) \quad (4)$$

The effect of the focal plane mask (coronagraph) is to send the DC component of this light pass to the reference arm and the higher-order terms are sent to the science arm. At the re-imaged pupils in the science and reference arms, the electric fields in the pupils are given by:

$$\begin{aligned} E_{ref} &= A t_{APLC}(x, y) \\ E_{sci} &= A(\varepsilon + i\varphi) t_{APLC}(x, y) \end{aligned} \quad (5)$$

Before the beams are recombined, they are modified by a few other elements. The reference beam passes a phase-shifting mirror and then through a spatial filter. The spatial filter has the effect of passing the average amplitude of the phase-shifted beam and also producing a pupil-dependent amplitude transmission function of its own. The science beam is picked off by a spectrally neutral beamsplitter and then recombined at the calibration beamsplitter. Putting all of these terms together leads to the following expression for the electric fields:

$$\begin{aligned} E_{ref} &= A \langle t_{APLC} \rangle e^{i\theta} t_{pinhole}(x, y) \frac{1}{\sqrt{2}} \\ E_{sci} &= A(\varepsilon + i\varphi) t_{APLC}(x, y) r_{sciBS}(x, y) \frac{1}{\sqrt{2}} \end{aligned}$$

We next make the simplifying assumption that the transmissions and reflections affect only the amplitude of the electric fields and not the phases ( $r$  and  $t$  are real numbers only) then we can represent them as the square-root of the intensity reflection/transmission ( $R$  and  $T$ ).

$$\begin{aligned} E_{ref} &= A \sqrt{\langle T_{APLC} \rangle} e^{i\theta} \sqrt{T_{pinhole}(x, y)} \frac{1}{\sqrt{2}} \\ E_{sci} &= A(\varepsilon + i\varphi) \sqrt{T_{APLC}(x, y)} \sqrt{R_{sciBS}} \frac{1}{\sqrt{2}} \end{aligned}$$

The intensity is then the absolute value of the sum of the electric fields.

$$\begin{aligned} E_{final} &= E_{ref} + E_{sci} \\ I_{final} &= E_{final} E_{final}^* \\ I_{final} &= \frac{1}{2} A^2 \left( \langle T_{APLC} \rangle T_{pinhole}(x, y) + T_{APLC}(x, y) R_{sciBS} (\varepsilon^2 + \varphi^2) + \right. \\ &\quad \left. 2 \sqrt{\langle T_{APLC} \rangle} \sqrt{T_{pinhole}(x, y)} \sqrt{T_{APLC}(x, y)} \sqrt{R_{sciBS}} \varepsilon \cos(\theta) + \right. \\ &\quad \left. 2 \sqrt{\langle T_{APLC} \rangle} \sqrt{T_{pinhole}(x, y)} \sqrt{T_{APLC}(x, y)} \sqrt{R_{sciBS}} \varphi \sin(\theta) \right) \end{aligned}$$

We now take four different phase-shifted images with phase values of  $\theta = 0, \pi/2, \pi, 3\pi/2$ . If we call the corresponding pupil images I1, I2, I3 and I4, then is possible to determine

the pupil-dependent residual phase and amplitude errors.

$$\begin{aligned} \varepsilon(x, y) &= \frac{I_1 - I_3}{2I_0 \sqrt{\langle T_{APLC} \rangle} \sqrt{T_{pinhole}(x, y)} \sqrt{T_{APLC}(x, y)} \sqrt{R_{sciBS}}} \\ \varphi(x, y) &= \frac{I_2 - I_4}{2I_0 \sqrt{\langle T_{APLC} \rangle} \sqrt{T_{pinhole}(x, y)} \sqrt{T_{APLC}(x, y)} \sqrt{R_{sciBS}}} \end{aligned}$$

## 4. THE CORONAGRAPH WAVE-FRONT SENSOR TESTBED

In order to test the principles of interferometric wave front sensing, we have constructed a testbed. It will allow us to test algorithms for wave front control. We will also be able to explore sensitivity, accuracy and systematic effects that set the limit on measurement accuracy.

A schematic of the testbed is shown below in Fig. 2. The coronagraph of choice for this setup was the apodized-pupil Lyot coronagraph. It will be used for the starlight suppression system for the Gemini Planet Imager Project.

First, we begin with a top level overview of the calibration system optics. In the optical layout shown below, we trace the rays from the location of the apodized pupil plane through to the final focal plane array of the HOWFS. In the science arm, the input pupil is re-imaged by the science re-collimation parabola to a location near the vertex of the merge prism. The HOWFS optical train will be described and detailed starting from this location to the final focal plane pupil image. On the reference arm side, the input pupil is re-imaged to a location roughly 75 mm behind the front surface of the LOWFS beamsplitter: a very convenient location. The pinhole camera images light that is reflected from the back side of the spatial filter pinhole with a simple finite-conjugate relay to give the appropriate The nulling interferometer and calibration system interferometer share a common beam splitter: the re-combination beam splitter of the nulier is the input beam splitter for the calibration system. The bright (asymmetric) port of the nulier passes through a spatial filter that removes any wave front errors in the system up to the pinhole. It is then re-collimated to form the reference arm of the calibration interferometer. A subsequent calibration phasing mirror allows this reference wave front to be phase shifted. The other arm of the calibration interferometer is created from a beam that is sampled from the science path by a spectrally-neutral beam splitter. This light also passes through an identical pair of OAP's. This is a simple way of both matching the polarization properties and path length of the beam that is in the reference arm.

As mentioned previously, the optical layout of the HOWFS sub-element will begin at the location of the re-imaged pupil which occurs after the beams have been re-combined. This pupil is formed very near to vertex of the merge prism. Now, there are some optical matters that need to be addressed before the re-combination beamsplitter, and this is because the calibration HOWFS is a broad-band, white-light, phase-shifting interferometer. For the interferometer to perform properly, it's internal optical paths, as a function of wavelength, from the point of separation at the focal-plane mask to the point of recombination must match to within a small fraction of a micron. This puts a constraint on the allowable dispersion (differential glass thickness) and DC phasing between the two arms of the interferometer. An interferometer is also sensitive to internal optical pathlength disturbances. In our case, these pathlength vibrations are only problematic when they are near the demodulation frequency. If they are at a higher frequency, they will average out during the integration time of a single measurement, while if they are slower, they will be frozen out. We have designed the optical beam height (and mechanical mounts) from the mounting surface to be small so as to increase the any mount-related resonant frequency.

Since we're working on a broadband astronomical instrument, atmospheric refraction is of necessity a concern. Left uncorrected, the residual atmospheric refraction will produce a chromatic smearing in the image plane and chromatic shear in the pupil plane. Both of these would have detrimental effects on the performance of both the LOWFS and HOWFS. The ADC has been added to mitigate against these effects. All of these optical aspects have been addressed before the HOWFS relay.

The layout of the HOWFS optical relay is shown above. The pupil is traced from the upper left. The pupil size is ten millimeters in diameter and the separation is designed such that upon demagnification, the two pupil images are on separate readout quadrants of the PICNIC array. The HOWFS fold mirror redirects the light to the HOWFS pupil lens. This lens is designed such that the input pupil is located at the back focal length so it is imaged to infinity. At the front focus of this lens is located the anti-aliasing spatial filter. The HOWFS pupil lens is a triplet designed to give good, broadband imaging from  $0.9 \mu\text{m} - 2.4 \mu\text{m}$ . The lens materials are common for the visible/near-infrared and the lens surface shapes are plano-spherical.

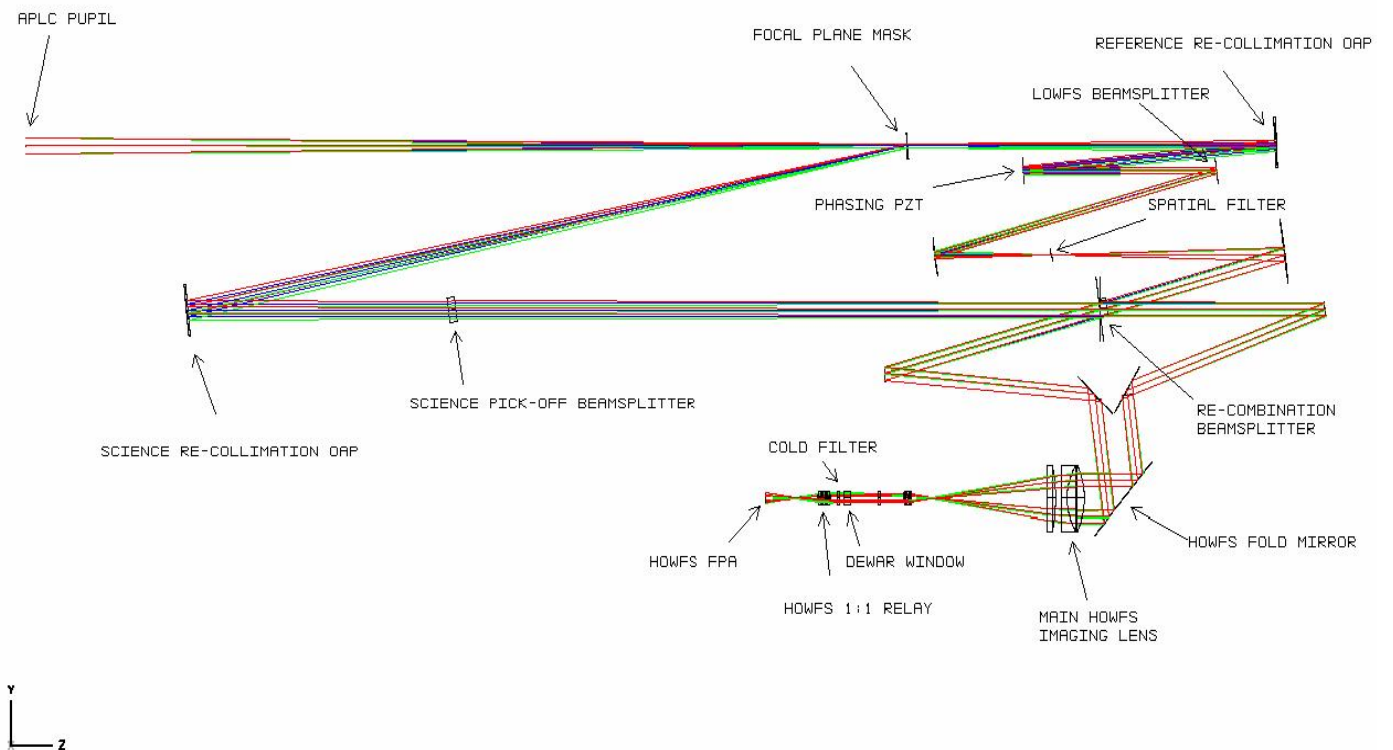


**Figure 2** – Schematic diagram of the calibration wave front sensing testbed for developing the hardware and algorithms used for interferometric wave front sensing.

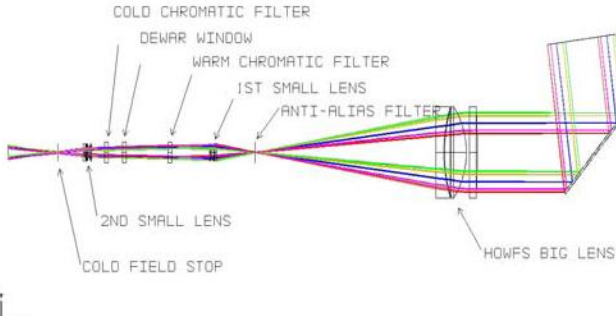


**Figure 3** – Schematic layout of the Gemini Planet Imager (GPI) Calibration wave front sensor.

The next optical element is the pupil re-imaging lens. It is also a triplet based upon the design of the HOWFS pupil lens. In the space before this lens, the pupil is at infinity, so after this lens it is re-imaged to the back focal length and de-magnified to the size and separation that will occur on the final image plane. This pupil image is formed near the location of the warm chromatic filters, this is advantageous as it makes the final image location of the focal plane array insensitive to the wedges in the warm chromatic filters. These filters contain the exact spectral filters as defined by the IFS plus a few neutral density filters for doing some calibrations without the focal plane mask. After the warm chromatic filters are the dewar window and the cold chromatic filter. The cold chromatic filter suppresses light longward of  $2.4 \mu\text{m}$  to mitigate the noise from the emissivity of warm filters.

The final lens in the HOWFS relay is the 1:1 imaging lens that relays the real, de-magnified imaged to the final focal plane. This lens is also a triplet, it's a symmetric design with only two common glasses and three unique radii of curvature so we don't anticipate that it will be difficult to manufacture. Between this lens and the focal plane is a cold field stop that is oversized from the anti-aliasing filter, but small enough to still significantly limit the solid angle seen by each pixel. This cold stop will be thermally tied to the cold finger of the cryo-cooler to give a temperature close to 80K.

In the reference arm of the calibration system, a real pupil image is formed approximately 75 millimeters after the LOWFS pick-off beamsplitter. The optical layout for the LOWFS, a traditional Shack-Hartman, is shown in the image below:

The two lenses are off-the-shelf and serve to compress the beam to the appropriate size for the lenslet array. The lenslet is also off-the-shelf and samples the pupil with an array of 7x7 subapertures. These spots are then imaged directly onto the final Shack-Hartmann sensor. A geometrical optics

analysis of this wavefront sensor is only useful for get pupil locations and sizes correct. The sensor works by measuring tilts in diffraction PSF's and has been modelled extensively and this work is described in the performance simulation section. A qualitative image of the final focal plane spots is given below so that one can appreciate the effect of the appodized pupil on the relative illumination of the sub-apertures.

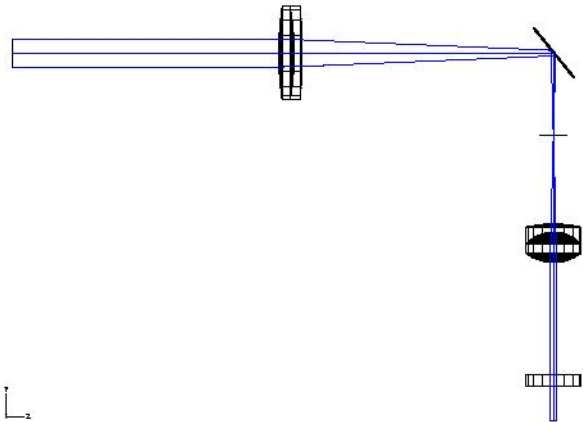


**Figure 4** – Schematic lay out of the Gemini Planet Imager (GPI) Calibration wave front sensor.

## 5. PRELIMINARY RESULTS

The testbed is now fully assembled and aligned, and we are getting some preliminary measurements from both the nulling interferometer and the calibration testbed. In order for the calibration algorithm to behave properly, the wave front errors into the calibration instrument must be small. Thus the first challenge is to produce a flat wave front from the nulling using the DM internal to one of the arms of the interferometer. Figure 4 above is a measurement of the phase shifted images through the nuller alone that are then used, in closed loop to flatten the wave front.

This first stage of the alignment algorithm is now working well, and after a couple of iterations converges properly. We are now exercising the calibration hardware and algorithm. Phase shifting on the calibration arm has been demonstrated and we are in the early stages of estimating the phase and extracting a phase correction to the DM. The goal is that once the null condition of the coronagraph has been established, we can sense and correct small phase errors using only the calibration system.

## 8. ACKNOWLEDGEMENTS

## 6. FUTURE WORK

As mentioned earlier, the goal of speckle calibration is critical for the future of direct detection of extra-solar planets. The work described here has been in support of the Gemini Planet Imager Instrument that is currently in the early planning stages. The coronagraph for this instrument will be an apodized pupil Lyot coronagraph: fundamentally, a much different coronagraph than the one used in the testbed described above. However, we have designed a calibration system that is compatible with this instrument and its requirements.

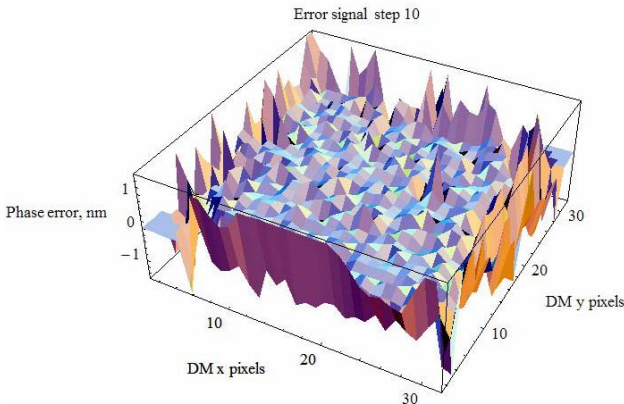


**Figure 5** – Preliminary data from the calibration testbed. This is a phase map of a DM surface being controlled with the (GPI) Calibration wave front sensor.

## 7. CONCLUSION

A method to suppress image plane speckles for planned and future planet-finding instruments has been described. We have also shown that the means by which phase and amplitude errors leak through a classic coronagraph and nulling coronagraph are fundamentally the same. A laboratory experiment to demonstrate this method is currently under development and showing early results. This calibration system is compatible with both imaging and nulling coronagraphs. Lessons learned from this work will be used in the development of the calibration system for the Gemini Planet Imager: GPI.

This work was carried out by the Jet Propulsion Laboratory, California Institute of Technology, under contract with the National Aeronautics and Space Administration. This work has been supported in part or full by the National Science Foundation Science and Technology Center for Adaptive Optics, managed by the University of California at Santa Cruz under cooperative agreement No. AST-9876783

## REFERENCES

- [1] B. Macintosh, et. al., The Gemini Planet Imager, Proc SPIE, Astronomical Telescopes and Instrumentation, these proceedings.
- [2] [http://planetquest1.jpl.nasa.gov/atlas/atlas\\_search.cfm](http://planetquest1.jpl.nasa.gov/atlas/atlas_search.cfm)
- [3] J. Goodman, *Introduction to Fourier Optics*, 2<sup>nd</sup> Ed., p.220, McGraw-Hill, 1996.
- [4] S. Shaklan, D. Moody, and J. Green. Residual Wave Front Phase Estimation in the Reimaged Lyot Plane for the Eclipse Coronagraphic Telescope. Proc. SPIE vol. 4860 (Waikoloa, 2002).
- [5] O. Guyon, “Imaging Faint Sources within a speckle halo with synchronous interferometric speckle subtraction”, *ApJ*, 615, 562-572, 2004.
- [6] J. Codona & R. Angel, *ApJL*, 604, L125, 2004.
- [7] K. Creath, “Phase-measurement interferometry techniques,” in *Progress in Optics XXVI*, E. Wolf, ed. (Elsevier, New York, 1988), Chap. 5.

## BIOGRAPHY



Kent Wallace is a Senior Optical Engineer at the Jet Propulsion Laboratory. He has been involved in the design and development of several ground based instruments including the Palomar Testbed Interferometer, the Keck Interferometer and the Palomar Adaptive Optics System. His interest over the past few years has been nulling interferometry, optical communications, and wave front sensing. He has a BS in Physics from Rose-Hulman Institute of Technology (in beautiful, suburban Terre Haute, IN) and a MS in Optics from the University of Rochester.